

Guided acoustic wave Brillouin scattering in photonic crystal fibers

Jean-Charles Beugnot, Thibaut Sylvestre, and Hervé Maillotte

Département d'Optique P. M. Duffieux, Institut FEMTO-ST, Centre National de la Recherche Scientifique UMR 6174, Université de Franche-Comté, 25030 Besançon, France

Gilles Mélin

Alcatel Research and Innovation, Route de Nozay, F-91460 Marcoussis, France

Vincent Laude

Département LPMO, Institut FEMTO-ST, Centre National de la Recherche Scientifique UMR 6174, Université de Franche-Comté, 25044 Besançon, France

Received June 20, 2006; revised October 2, 2006; accepted October 2, 2006; posted October 16, 2006 (Doc. ID 72077); published December 13, 2006

We experimentally investigate guided acoustic wave Brillouin scattering in several photonic crystal fibers by use of the so-called fiber loop mirror technique and show a completely different dynamics with respect to standard all-silica fibers. In addition to the suppression of most acoustic phonons, we show that forward Brillouin scattering in photonic crystal fibers is substantially enhanced only for the fundamental acoustic phonon because of efficient transverse acousto-optic field overlap. The results of our numerical simulations reveal that this high-frequency phonon is indeed trapped within the fiber core by the air-hole microstructure, in good agreement with experimental measurements. © 2006 Optical Society of America
OCIS codes: 060.4370, 290.5830.

Forward or guided acoustic wave Brillouin scattering (GAWBS) has recently been investigated in photonic crystal fibers (PCFs) because of their intriguing acoustic properties.^{1–3} The periodic wavelength-scale air-hole microstructure of solid-core PCFs can indeed drastically alter the transverse elastic waves distribution, and therefore forward Brillouin scattering, compared with what is commonly observed in conventional all-silica fibers. For instance, it was reported in Ref. 1 that the shear velocity, and therefore the acoustic frequency, decreases with the air-filling fraction. Strong reduction of GAWBS has been observed in a broad frequency range up to 400 MHz,² thus paving the way for PCF-based quantum optics experiments. Using a photoacoustic pump-probe technique, Dainese *et al.*³ showed very recently that only a few high-frequency acoustic phonon modes are generated in ultrasmall-core PCFs as a result of phononic bandgaps, which is reminiscent of a Raman-like scattering process. In this Letter, polarized GAWBS in several PCFs is experimentally investigated using the so-called fiber loop mirror technique.⁴ Our experimental observations also confirm the existence of strong transverse acoustic phonons in the GHz range, highlighting the completely different dynamics compared with those of standard all-silica fibers. Using a finite element method,⁵ we show that these acoustic phonons are trapped within the small PCF core by the air-hole cladding structure without phononic bandgaps. Thanks to a strong acousto-optic transverse field overlap, GAWBS in PCFs is therefore substantially enhanced for the fundamental acoustic phonon core

Let us recall that polarized GAWBS in an optical fiber results from the radial dilatation or R_{0m} modes,

which causes pure phase modulation noise.⁶ To observe this effect, we set up an optical interferometer such as the fiber loop mirror depicted in Fig. 1.⁷ As a pump laser, we used a distributed-feedback erbium fiber laser emitting at a wavelength of 1549.94 nm and with a linewidth below 45 kHz. It is then amplified by a high-power erbium-doped fiber amplifier (EDFA) and filtered by a 5 nm bandpass filter. The light is then split into two counterpropagating beams by a 50/50 coupler. The GAWBS-induced phase modulation is then converted to amplitude modulation at the fiber loop mirror output by optimizing the interferences with the input polarization controller (polar contr). The GAWBS spectra are then recorded over a broad frequency range of up to 1400 MHz by an electrical spectrum analyzer. We performed the measurements in three different small-core PCFs [see the insets in Figs. 2(a)–2(c) for a cross section and Table 1 for detailed characteristics]. As a comparison, we also performed GAWBS measurements in a long conventional dispersion-compensating fiber (DCF). The results of all measurements are presented in Fig. 2. As can be seen, all three PCFs exhibit GAWBS spectra completely different from that of the DCF [Fig. 2(d)], for which a set of acoustic phonon modes is generated over a broad frequency range

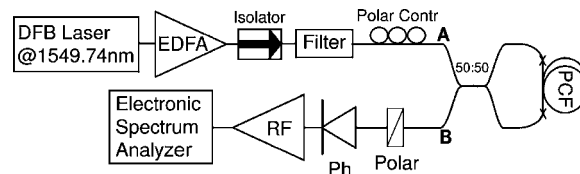


Fig. 1. Experimental setup for polarized GAWBS measurement with a fiber loop mirror. Polar, polarizer; Ph, photodetector; RF, RF amplifier. Other abbreviations defined in text.

Table 1. Parameters of the PCFs Under Test^a

Characteristics	PCF70	PCF8	PCF4	DCF
Core diameter (μm)	11	3.9	2.4	—
Pitch, Λ (μm)	8.1	4.1	2.8	—
d/Λ	0.59	0.84	0.84	—
Length (m)	400	98	44	5700
Cladding (μm)	125	175	175	125
A_{eff} (μm^2)	70	8	4	50
ν_a (MHz)	300	812	1281	—
ν_c (MHz)	1490	3730	5430	1200
ν_Λ (MHz)	375	730	1070	—

^a Λ , pitch; d , air-hole diameter. ν_c and ν_Λ are characteristic frequencies for the disappearance of GAWBS resonances defined in the text.

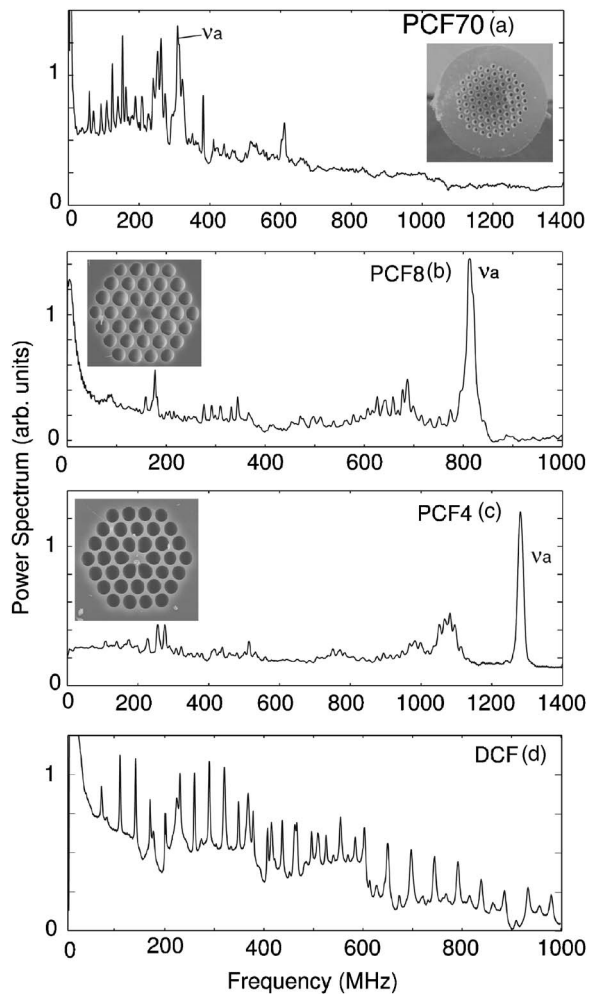


Fig. 2. Polarized GAWBS spectra of (a)–(c) three solid-core PCFs and (d) a DCF. The spectral resolution was 300 kHz. The insets show scanning electron microscope images of the cross sections.

of up to 1000 MHz.^{6,7} First, we can see a substantial reduction of GAWBS in PCFs compared with the conventional DCF, in good agreement with recent results.² Second, Figs. 2(b) and 2(c) clearly show the strong generation of an acoustic phonon in both PCF8 and PCF4 at frequencies of 812 and 1281 MHz, respectively. These two modulation frequencies present large Q factors, i.e., $\nu_a/\Delta\nu_a \approx 50$, where ν_a is

the acoustic frequency and $\Delta\nu_a$ is the full width at half-maximum. The generation of these isolated phonons in PCFs can be understood by considering the case of conventional fiber. GAWBS depend mainly on the fiber cladding diameter (typically 125 μm), which allows for a wide spatial domain of existence of acoustic modes.⁶ However, the optical mode is guided within the small core and only partially overlaps the GAWBS acoustic modes. In PCF, a strong dependence on additional boundary conditions is introduced due to the microstructured air-hole area, leading to the spatial redistribution of most acoustic phonons and to the strong confinement of some phonon modes within the PCF core. As a consequence, a large overlap factor between the transverse acoustic modes trapped in the core and the fundamental optical mode can be made possible thanks to the microstructuring, significantly enhancing the acoustic-optic wave interaction. On the other hand, the suppression of most of the GAWBS modes in the lower frequency range results from the fact that the mechanical coupling between core and cladding is significantly reduced by the air holes.² In PCF70, Fig. 2(a) shows that GAWBS resonances in this lower frequency range below 300 MHz are more closely spaced in PCFs compared with standard DCFs. Indeed, flexural and rotational acoustic modes cannot be observed in standard fibers (R_{0m} modes are purely dilatational). However, because of the air-hole cladding structure, no acoustic mode in a PCF is purely flexural, rotational, or dilatational, but all exhibit a variable amount of shear and longitudinal displacements.

We performed numerical calculations of acoustic phonon modes for our three PCFs using the finite element method (FEM) of Ref. 5. Figure 3 illustrates the evolution of the acoustic frequency as a function of the PCF core diameter. The measured acoustic frequencies (crosses) are also shown in this figure, and there is excellent agreement with the numerical calculations (circles). Figure 3 also shows in gray scale the elastic energy of the acoustic phonon trapped in the core of PCF8, which corresponds to the peak labeled ν_a in Fig. 2(b). This mode has been identified as

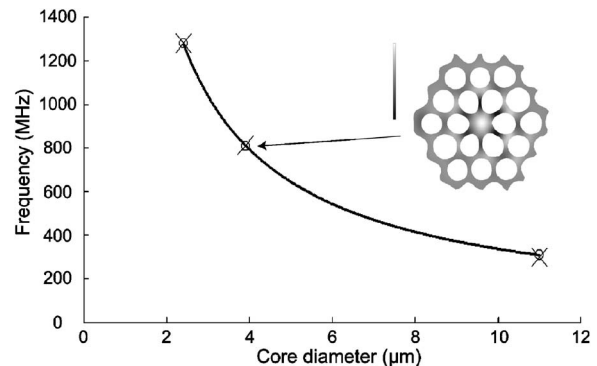


Fig. 3. Isolated acoustic mode frequency as a function of the PCF core diameter. Experimental measurements (crosses) and finite element method results (circles) and with a hyperbolic fit (solid curve). Inset, elastic energy of the fundamental longitudinal phonon mode localized in PCF8's core.

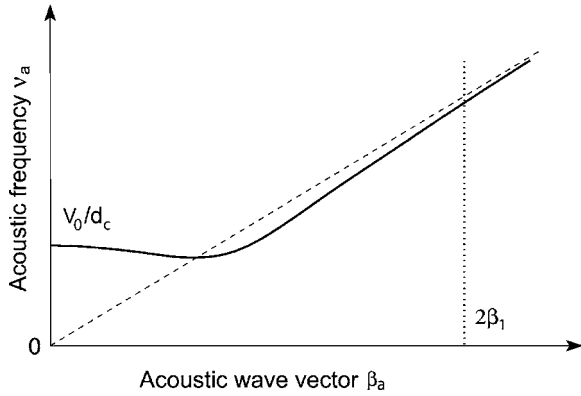


Fig. 4. Schematic of the dispersion of the fundamental longitudinal phonon confined in the core of a PCF (solid curve). The longitudinal line with slope $V=5970$ m/s is the asymptotic limit (dashed curve). $V_0=3200$ m/s, and d_c is the core diameter.

the fundamental longitudinal phonon mode of the core, which is strongly confined in the core by the air-hole microstructure, although a phononic bandgap effect is not at play, unlike the case considered in Refs. 3 and 5. We also found such a localized acoustic wave at a frequency of 300 MHz for the large-effective-area PCF70, in good agreement with the highest measured GAWBS frequency peak shown in Fig. 2(a). This acoustic mode is, however, less clearly distinguishable from the others in the GAWBS spectrum because the air-hole area in PCF70 is less favorable for acoustic guidance within the core than are PCF8 and PCF4. For all PCFs, it is significant that the product of the acoustic mode frequency by the core diameter is found to be a constant to a good approximation. The hyperbolic fit in Fig. 3 shows that this constant equals 3200 m s^{-1} .

Figure 4 sketches the dispersion of the fundamental phonon as a function of the longitudinal component of the acoustic wave vector, β_a . In forward Brillouin scattering, phase matching leads to the relations $\nu_2 - \nu_1 = \nu_a$, $\beta_2 - \beta_1 = \beta_a$, where ν_1 and β_1 (ν_2 and β_2) are the frequency and the wave vector, respectively, of the incident optical wave (diffracted optical wave). Because the acoustic frequency is always negligible with respect to optical frequencies, one has $\nu_2 \approx \nu_1$ and $\beta_2 \approx \beta_1$. Then β_a is small, although nonvanishing. As a result, the phonon is excited near its cutoff, as illustrated in Fig. 4. The same phonon would also be involved in backward Brillouin scattering, but at another point of its dispersion branch. In this case, phase matching implies that $\nu_2 - \nu_1 = \nu_a$, $\beta_2 + \beta_1 = \beta_a$, and the same argument as above leads to $\beta_a \approx 2\beta_1$. For large β_a , the phonon frequency tends to the longitudinal asymptotic limit, as usual with backward Brillouin scattering in fibers.

The fact that phonons confined to the core are predominant in GAWBS spectra can be explained by examining the elasto-optic diffraction coefficient given by⁵

$$\kappa = \int E_{1i} E_{2j}^* p_{ijkl} S_{kl} d\mathbf{r}, \quad (1)$$

with the integral taken over the fiber cross section. E_1 and E_2 are the electric field vectors of the incident and the diffracted optical modes, respectively; p_{ijkl} is the elasto-optic tensor; S_{ij} is the phonon strain tensor; and the repeated index summation convention is implied. Equation (1) obviously implies that the phonon modal shape should resemble that of the optical modes guided in the core. In addition, it can be used qualitatively to understand the gradual disappearance of GAWBS resonances as the frequency increases, as can be observed in Fig. 2. κ will tend to zero when the phonon mode has several nodes within the optical effective area. Defining an effective radius, r_{eff} , through $A_{\text{eff}} = \pi r_{\text{eff}}^2$, we define a first limiting frequency $\nu_c = V/r_{\text{eff}}$ with $V=5970$ m/s the longitudinal velocity in silica. Above ν_c , at least two acoustic wavelengths fall radially within the optical effective area. In the case of PCFs, we define a second limiting frequency $\nu_\Lambda = V/(2\Lambda)$. Above ν_Λ there is strong interference of acoustic waves scattered by the holes. This leads to strong redistribution of acoustic energy and the appearance of nodes within the core for most GAWBS phonons. Table 1 indicates that ν_c is the limiting frequency for the DCF, while ν_Λ is the limiting frequency for all PCFs.

In conclusion, we have experimentally reported that guided acoustic wave Brillouin scattering in solid-core photonic crystal fibers is substantially increased for the fundamental acoustic phonon mode. Numerical investigations have shown that the air-hole cladding structure of PCFs indeed allows for the trapping of this fundamental acoustic phonon within the core with an efficient transverse field overlap. This has been confirmed by the fact that the numerically calculated acoustic frequency is in good agreement with measurements. This effect may have potential applications to novel Brillouin-based optical devices, since the PCF acts as an efficient phase modulator, or more generally to the generation of coherent acoustic waves.

This work has been supported by the Ministère Délégué à la Recherche. J.-C. Beugnot's e-mail address is jean-charles.beugnot@univ-fcomte.fr.

References

1. N. Shibata, A. Nakazomo, N. Taguchi, and S. Tanaka, *IEEE Photon. Technol. Lett.* **18**, 412 (2006).
2. D. Elser, U. L. Andersen, A. Korn, O. Glöckl, S. Lorenz, Ch. Marquardt, and G. Leuchs, *Phys. Rev. Lett.* **97**, 133901 (2006).
3. P. Dainese, P. St. J. Russell, G. S. Wiederhecker, N. Joly, H. L. Fragnito, V. Laude, and A. Kelif, *Opt. Express* **14**, 4141 (2006).
4. N. J. Doran and D. Wood, *Opt. Lett.* **13**, 56 (1988).
5. V. Laude, A. Khelif, S. Benchabane, M. Wilm, T. Sylvestre, B. Kibler, A. Mussot, J. M. Dudley, and H. Maillotte, *Phys. Rev. B* **71**, 045107 (2005).
6. R. M. Shelby, M. D. Levenson, and P. W. Bayer, *Phys. Rev. B* **31**, 5244 (1985).
7. N. Nishizawa, S. Kume, M. Mori, T. Goto, and A. Miyauchi, *Opt. Lett.* **19**, 1424 (1994).